

U. S. DEPARTMENT OF THE INTERIOR

U. S. GEOLOGICAL SURVEY

Application of Nonlinear Dynamics to Understanding Earthquake  
Sequences in Time and Space: G. K. Gilbert Fellowship Report

by

David J. Varnes<sup>1</sup> and Charles G. Bufe<sup>1</sup>

Open-File Report 95-60

This report is preliminary and has not been reviewed for conformity with U. S. Geological Survey editorial standards (or with the North American Stratigraphic Code). Any use of trade, product, or firm names is for descriptive purposes only and does not imply endorsement by the U. S. Government.

<sup>1</sup> U. S. Geological Survey, Golden, Colorado

## Abstract

Almost all natural phenomena are controlled by nonlinear processes, in which output is not in simple linear proportion to input. In dynamics, nonlinearity means that measured properties of a system at a late time,  $T_2$ , depend on the value of those properties at an earlier time,  $T_1$ , in relations that cannot be expressed as a simple proportion or as differing by a constant. Dynamical systems are best defined mathematically by differential equations, but there are no general procedures for solving nonlinear differential equations. Hence, with few exceptions, they can be approximated only by numerical methods. Moreover, in the last few decades, it has been found that some simple nonlinear relations, even though they evolve into future states that are completely determined by the rules of those relations, can nevertheless produce outputs that are wholly or in part very irregular and apparently random.

### Nonlinear Failure Processes

In our research we have sought to determine whether some seismic series follow nonlinear relations that may result from an underlying deterministic rather than a truly random process. Because seismicity in the brittle part of the lithosphere reflects a process of material failure, we have applied to the analysis of seismic series one of the more successful relations developed over many decades of research on the failure of metals and earth materials. The relation used is a simple first-order nonlinear differential equation,

$$\frac{d\Omega}{dt} = \frac{C}{(t_f - t)^{1-m}} \quad (1)$$

where  $\Omega$  represents the measure of some accelerating quantity in a progressively deforming body such as displacement, strain, or accumulated emitted energy;  $t$  is the time at which an observation of  $\Omega$  is made;  $C$  and  $m$  are constants; and  $t_f$  is the expected time of catastrophic failure. This is known as a generalized Saito equation, after a prominent Japanese engineer, and in seismology as an INPORT relation from Inverse Power Of Remaining Time (Varnes, 1989).

Although relations of the form of equation (1) were derived in part empirically by engineers, they have a basis in both experiment and physical theory going back many decades. In relation to seismology, equation (1) also can be derived by extending the work published by Das and Scholz (1981) on crack propagation. Such a relation describes the growth of a circular plane shear crack in an infinite homogeneous medium, subject to constant boundary stress during the final part of the nucleation phase preceding instability.

We have found that many precursory seismic sequences that culminated in large earthquakes follow the INPORT relation closely, particularly if  $\Omega$  in equation (1) is chosen to represent Benioff strain release ( $\sqrt{M_o}$ ) where  $M_o$  is seismic moment. Either equation (1), or the integrated form used when the accumulated release of seismic moment is computed, can be fit to precursory seismic sequences in a computer program

developed by C. G. Bufe. This program takes as input the magnitude and times of earthquakes in a series that might be precursory to a large event and determines the values of  $C$ ,  $m$ , and  $t_f$  that yield the best fit in nonlinear regression. The exponent  $m$  can be solved for, or, if it appears to be relatively constant in a region,  $m$  may be fixed and attention directed to the detailed variation of  $t_f$  as affected by progressively accumulating data with the passage of time. Under certain conditions the magnitude as well as the time of a culminating event can be estimated. However, the computer search may not converge to a stable solution and the trial fails if the series does not accelerate according to equation (1).

In our application of the INPORT relation to seismicity of the greater San Francisco Bay region we found that, in general, the best results were obtained when  $\Omega$  represented the square root of moment. Eighteen analyses were completed of  $M \geq 5$  to  $M \geq 5.5$  earthquakes during various time intervals between the mid 1800's and 1989, and within all or parts of adjoining  $1 \times 2$  degree rectangular areas between latitudes 36.5 and 39.5 N in coastal California. Seismicity during the latter part of the 19th century preceding the 1906 great earthquake was used to determine a regional value of  $m$ . This  $m$  was used to analyze the generally accelerating seismicity between 1927 and 1989. In an area that included all three quads, the best fit yielded  $t_f = 1990.0$  and  $M = 6.8$  (see Figure 1). For the southern of the three quads, which is practically centered on Loma Prieta, the solution yielded  $t_f = 1989.9$  and  $M = 6.3$ . The actual Loma Prieta event occurred at 1989.8 and had magnitudes  $M_L = 6.7$  and  $M_S = 7.1$ . By splicing pre-1906 and post-1906 accelerating curves for northern California seismicity, the span of the total seismic cycle between events of the 1906 earthquake magnitude was estimated at  $269 \pm 50$  years. The method and results of analyses of seismicity in northern coastal California have been published earlier (Bufe and Varnes, 1993).

Similar methods were also applied to analysis of seismicity in the Alaska-Aleutian subduction zone (fig. 2). The high likelihood of a gap-filling thrust earthquake within this decade is indicated both by the historic earthquake recurrence data and by the nonlinear dynamics of the INPORT analysis applied to recent decades of instrumental data. May 1993 earthquake activity in the Shumagin Islands gap is consistent with previous projections of increases in seismic energy release, indicating that this segment, along with the Alaska Peninsula segment, is approaching failure. Based on this pattern of accelerating seismic release, we project the occurrence of one or more  $M \geq 7.3$  earthquakes in the Shumagin-Alaskan Peninsula region during 1994-1996. Other zones currently showing accelerating release are the Delarof and Kommandorski segments. Time-to-failure analysis suggests that large earthquakes could occur in these zones within the next few years (Bufe, Nishenko, and Varnes, 1994).

Part of our work was on analysis of a precursory seismic series in the Caribbean near the Virgin Islands. Seismic activity in the 10 months preceding the 14 February 1980,  $m_b$  4.8 earthquake was reported on by Frankel in 1982. We found that the seismic activity consisted of 4 principal cycles, that each cycle began with an episode of closely timed events including a relatively large event, and that each cycle was about  $3/4$  the

length of the preceding cycle. The last two episodes preceding the main shock were accompanied by the occurrence of events outside the study area at distances of less than 60 km from the main shock. These events were comparable in size ( $m_b$  4.6 and 4.7) to the main shock. This pattern (fig. 3) could have been used to predict the time of the end of the fourth cycle, but not that the cycle would be terminated by a much larger event, that is, the main shock. The expectation of the main shock was, however, indicated by application of a nonlinear time- and slip-predictable foreshock model developed by Bufe, Varnes, and Nishenko (1993). This model, applicable to those foreshock sequences in which larger foreshocks occur as time of failure is approached, was applied to the upper and lower bounds of the cumulated square root of seismic moment versus time plot (fig. 4). The best retrospective functional fit, represented by the lower- and upper-bound curves, describes the principal features of the sequence, projecting from the last datum, 43 days before the main shock, to an expected main shock of  $m_b$  4.5 (actual 4.8) at a time only 2 days later than the actual time.

### Properties of nonlinear dynamic systems

The above indications that the seismic series had an underlying regularity led us to apply some techniques for analyzing nonlinear dynamic systems to the Virgin Islands data. One method is to determine the dimension of a pertinent characteristic of the system. We chose the time between events as a precisely determined, observable characteristic of the system. In the classical concept, such a set of points defining times would have a dimension of zero. It turned out that all the possible 666 interevent times among the 37 earthquakes of the series formed a set with a non-integer correlation dimension of 0.7. This suggested that the seismic time series is temporally fractal. A similar examination of interevent hypocentral distances, which if nonfractal would have a dimension of 1, yielded a correlation dimension of 1.3, also suggesting that the seismic series is spatially fractal. These calculated dimensions are approximate, calculated from a relatively small data set, and are probably minimums, as they were determined from an irregular and discrete set of interevent times and distances.

Knowledge of a poorly understood process often can be advanced by disclosing patterns in the development or products of the process. One of the techniques used to reveal unsuspected patterns in analysis of discrete nonlinear dynamic systems is to iterate successive outputs. We have chosen, for example, to iterate successive rates of seismicity. The rate of occurrence of seismic events can be defined simply by the reciprocal of interevent time intervals between consecutive events. These successive rates,  $R_i$  and  $R_{i+1}$ , define points in 2-D log-log space, as shown in fig. 5. This diagram reveals some unexpected regularities: several families of parallel, or nearly parallel, lines connect successive data points. Even more striking are the similar geometric figures made by connecting the series of points in set 6, 7, 8, 9, 10 and in a second set of points 24, 25, 26, 27, and 28. These two sets, shown by heavy lines, are separated in time by a nearly constant interval of about 200 days, yet identify parallel sequences of events that are not apparent in the raw data.

The irregular spiral of Figure 5 can be expanded into 3 dimensions by plotting each point of the figure at the time  $t_i$  of the event that separates the intervals. Figure 6 is a projection of the resulting helix as viewed horizontally and in the direction indicated by the arrow in Figure 5. Now, more regularities become apparent concerning the times between events. If a certain interval of 140,488 minutes (97.56 days) is taken as a unit of measure, many other intervals between events are seen to be simple rational fractions of that unit. Each of those identified in the figure are accurate within one percent.

### Summary

We have shown that accumulated seismic strain release may follow determinable mathematical functions and that regularities in the times between precursory seismic events can be disclosed by iterative techniques used in nonlinear dynamics. Although the physical causes of these regularities are not clear, the presence of different types of regularities strongly suggests that at least some earthquake sequences are not random but result from underlying deterministic nonlinear physical processes. We believe analyses of these relations and regularities may lead to a better understanding of the dynamics of earthquake generation.

### References Cited

- Bufe, C. G., and Varnes, D. J., 1993, Predictive modeling of the seismic cycle of the greater San Francisco Bay region: *Journal of Geophysical Research*, v. 98, no. B6, p. 9871-9883.
- Bufe, C. G., Varnes, D. J., and Nishenko, S. P., 1993, A nonlinear time- and slip-predictable model for foreshocks (abstract): *EOS, Transactions, American Geophysical Union*, v. 74, p. 437.
- Bufe, C. G., Nishenko, S. P., and Varnes, D. J., 1994, Seismicity trends and the potential for large earthquakes in the Alaska-Aleutian region: *Pure and Applied Geophysics*, v. 142, no.1, Special Issue on Shallow Subduction Zones, R. Dmowska and G. Ekstrom, eds., p. 83-99.
- Das, S., and Scholz, C. H., 1981, Theory of time-dependent rupture in the Earth: *Journal of Geophysical Research*, v. 86, no. B7, p. 6039-6051.
- Jaume', S. C., 1992, Moment release rate variations during the seismic cycle in the Alaska-Aleutian subduction zone: extended abstract, *Proceedings, Wadati Conference on Great Subduction Earthquakes*, University of Alaska, Fairbanks, p. 123-128.
- Varnes, D. J., 1989, Predicting earthquakes by analyzing accelerating precursory seismic activity: *Pure and Applied Geophysics*, v. 130, no. 4, p. 661-686.

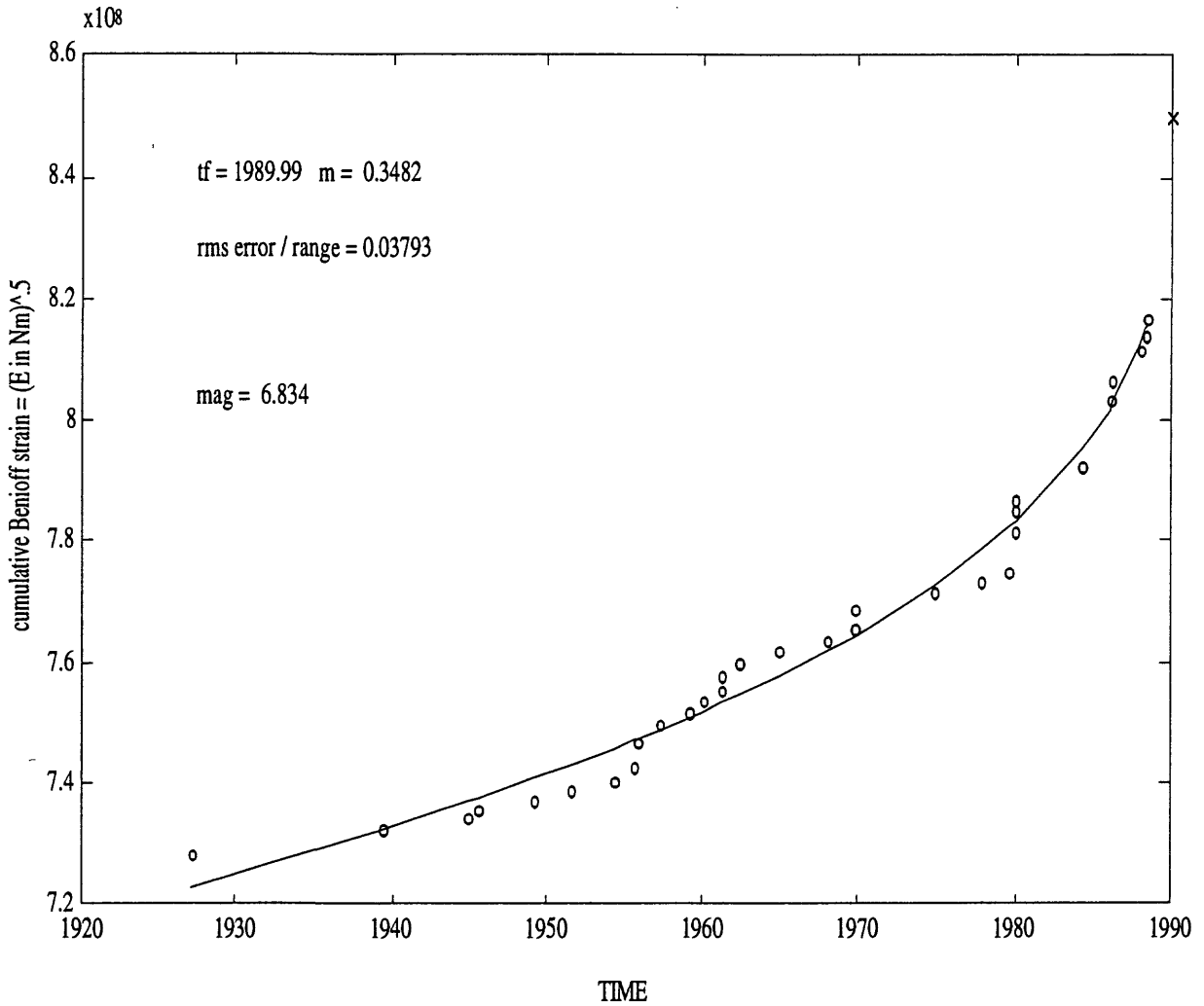


**Figure 1.** Cumulative (from 1855) pre-step values of Benioff strain release for northern California earthquakes of magnitude 5 or greater for the period 1927-1988. The line is the best fit solution for  $m$  and  $tf$ .

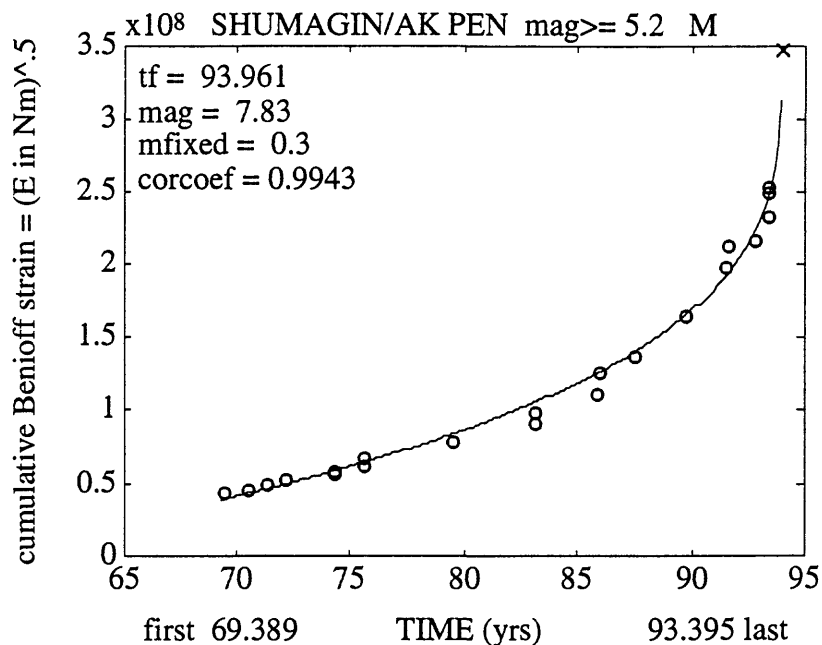


*Figure 2. Time-to failure analyses of cumulative Benioff strain for combined Shumagin Islands and Alaska Peninsula segments (155-162 W. longitude) using data for  $M_S \geq 5.2$  from an earthquake catalog developed by Steven Jaume' at Lamont-Doherty Earth Observatory (Jaume', 1992). Time is in years since 1900,  $t_f$  is projected time of failure, mag is projected moment magnitude, mfixed is exponent of time to failure, and corcoef is correlation coefficient for data fit.*

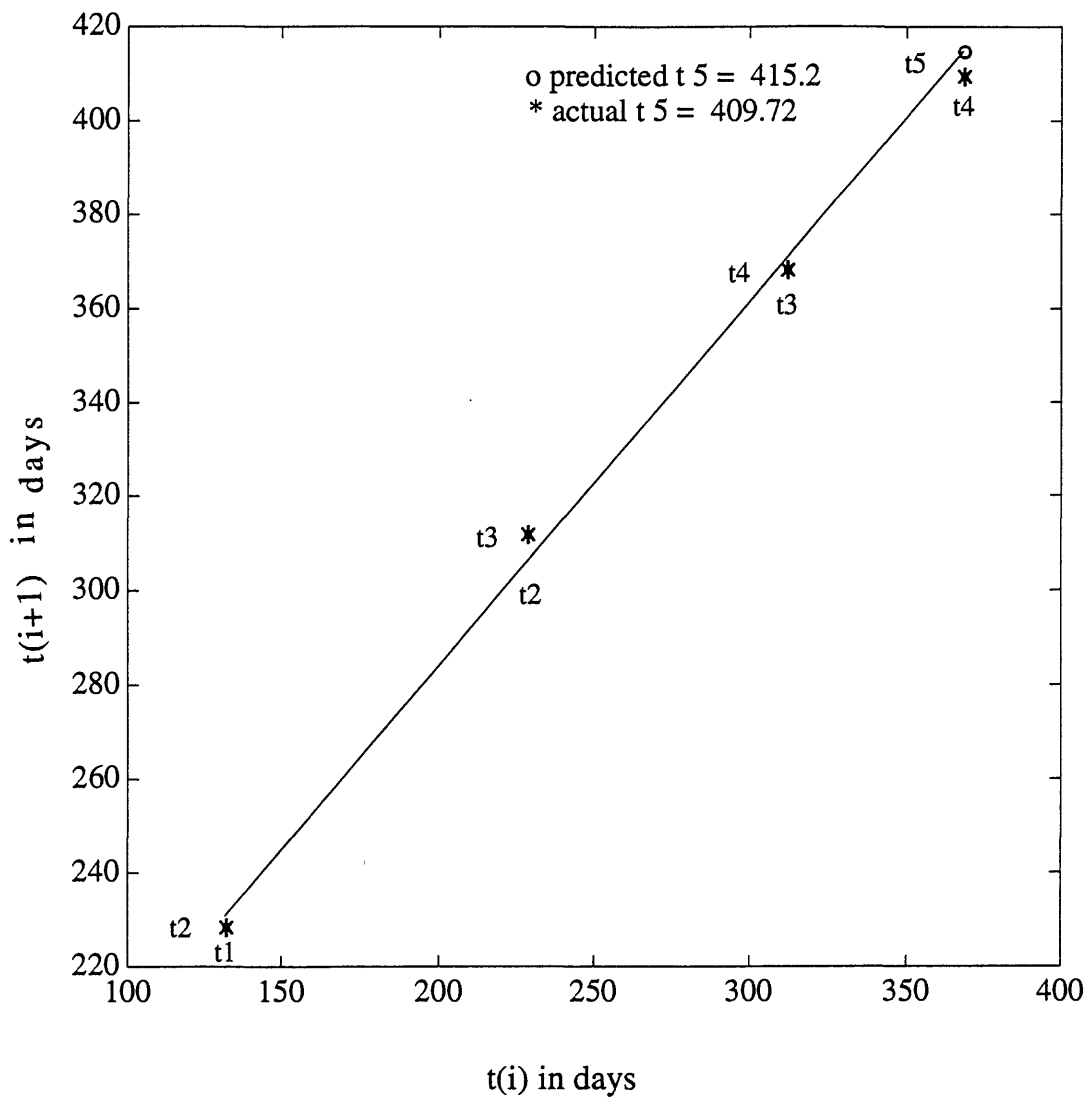
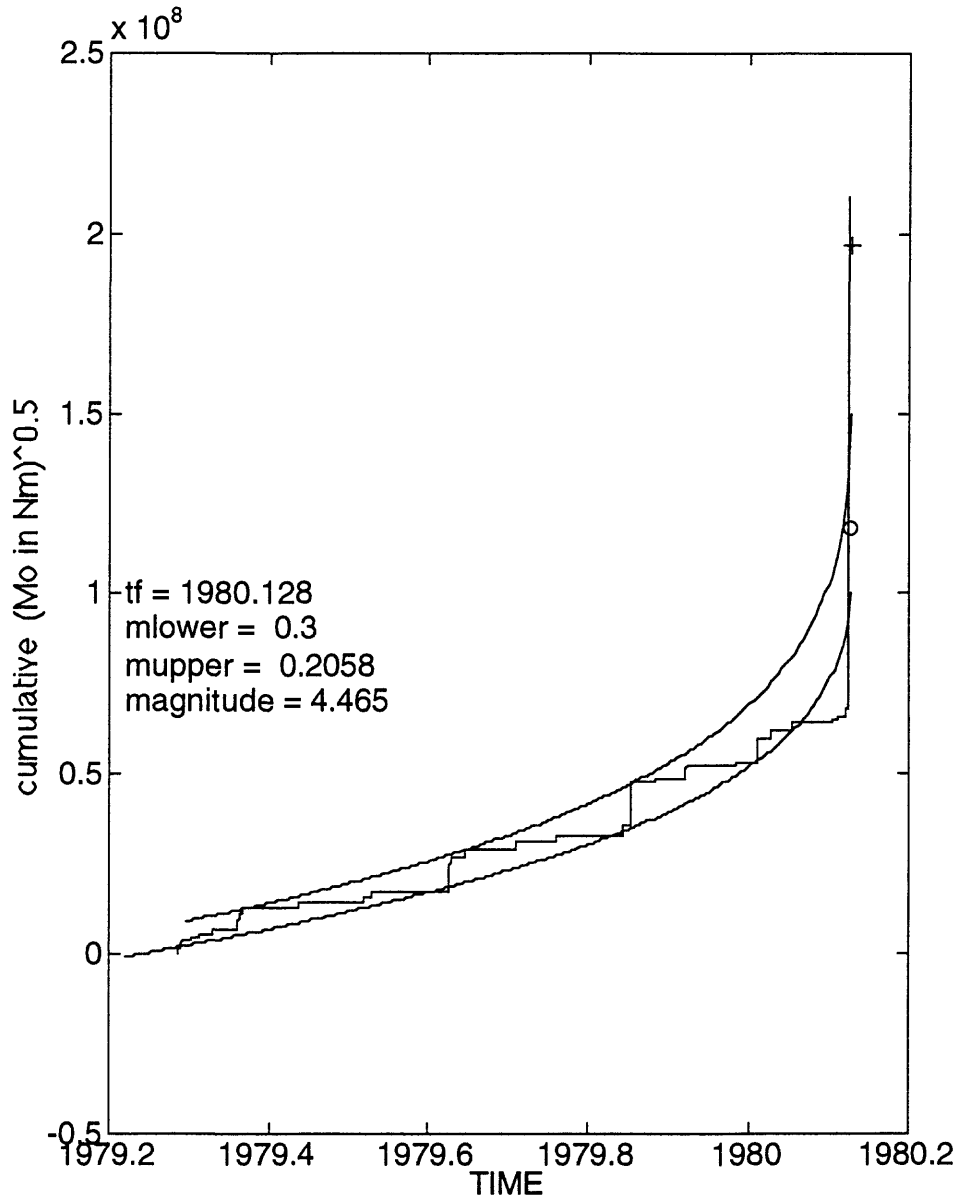
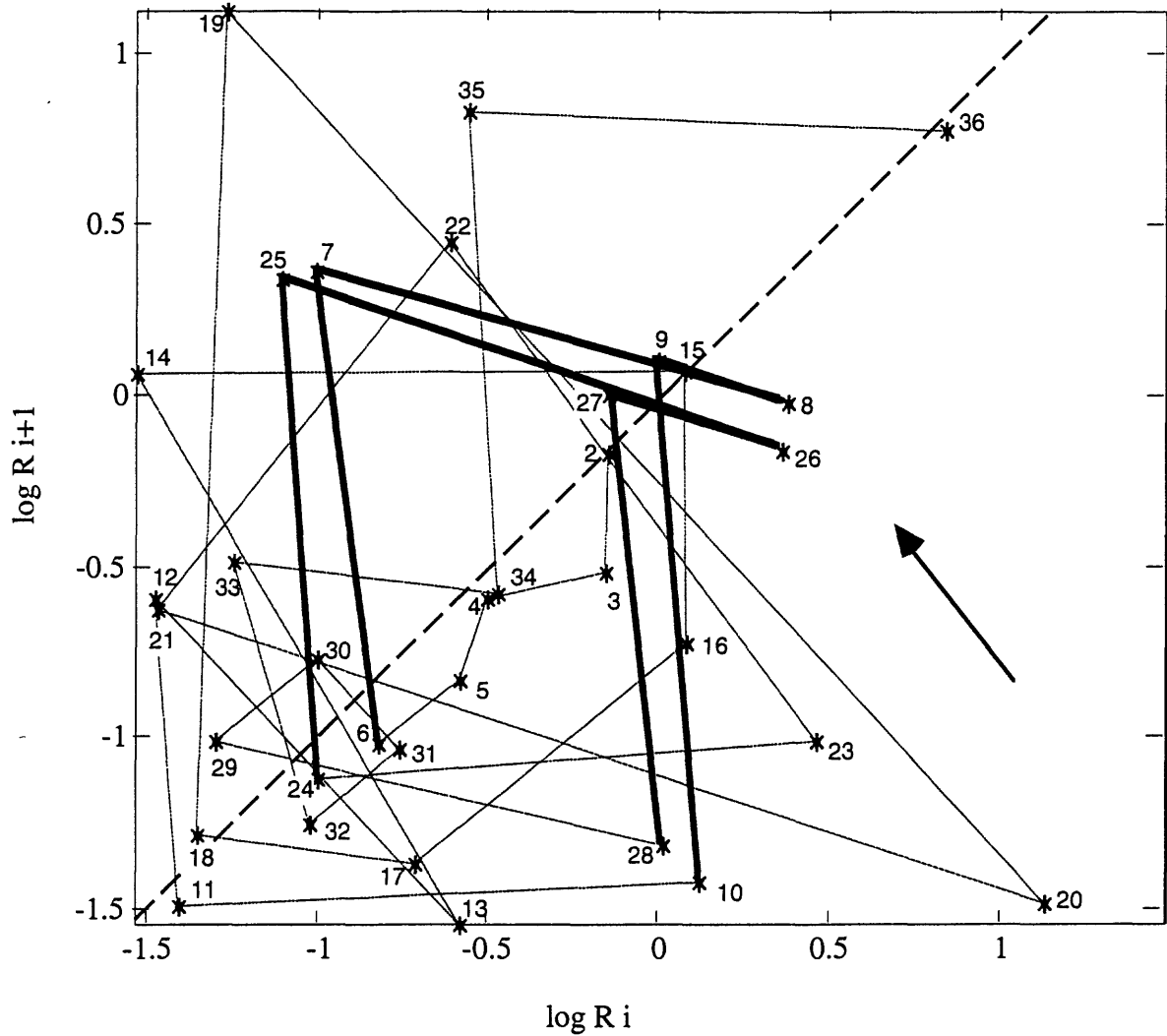


Figure 3. Times of principal intervals (largest event in cluster) form a linear plot when iterated one against the next. This allows prediction of the time of the main shock, but not its size.



*Figure 4. Stairstep graph of the accelerating increase of the cumulative square root of seismic moment released by the 37 events in the Virgin Islands sequence. The upper and lower bounds of the plot (values at  $t_f$  are shown as + and o, respectively) are confined within curves, described in the text, that lead to estimates of the time and magnitude of the main shock.*



**Figure 5.** Iteration of log rate of occurrence of successive seismic events. Rate is defined by the reciprocal of the time since the previous event. For example, the point labeled 10 is plotted at  $\log R_i = \log [1/(t_{10}-t_9)] = 0.112$ , and  $\log R_{i+1} = \log [1/(t_{11}-t_{10})] = -1.416$ , where  $t_9$ ,  $t_{10}$ , and  $t_{11}$  are the times of successive events since April 15, 1979. The heavier lines connecting points 6 through 10 and 24 through 28 indicate two similar successions of time intervals that occurred about 200 days apart. The arrow indicates the angle of view of Figure 6.

